## Ⅲ．ゲフィチニブ使用の動向

IDEALにより肺癌で一定の効果が認められたものの，その後，プラチナ製剤を含む化学療法へのゲフィチニブの上乗せ効果があるかを検討した第3相試験で有意差が得られなかったこと[11, 12]，また既治療進行非小細胞癌に対してのプラセボと比較した試験（ISEL，日本人は含まれていない）で有意な生存期間の延長が得られなかったことを受け[35]，米国食品医薬品局（FDA）は2003年5月に標準的化学療法不応の進行非小細胞肺癌に対しての単独使用を一旦は承認していたが，2005年6月からは新規使用を原則禁止している．

製造販売元であるアストラゼネカ社は欧州医薬審査局（EMEA）への承認申請を取り下げた．しかし，ISELにおけるサブセット解析で東洋人での生存期間延長を認め，さらに後述するゲフィチニブ感受性EGFR遺伝子変異が東洋人に多いことが報告されるに至り，現在も日本を含むアジア諸国を中心に承認，使用されている．

日本でのゲフィチニブ使用開始後に社会問題となった急性肺障害，間質性肺炎発症については，発症率は5.8％でその死亡率は2.3％とされ，喫煙歴を有するもの，PS＞2，間質性肺炎合併症例，男性等が危険因子とされる．現在，ゲフィチニブの使用については安全に使用するためのガイドラインが日本肺癌学会から公表されている[37]．

## Ⅳ．ゲフィチニブ感受性とEGFR変異との相関

ゲフィチニブの抗腫瘍効果については，当初EGFR発現量との相関が予想されたが，臨床試験における後ろ向き解析において否定された[4]．それらで明らかになったのは，非喫煙者，腺癌，女性，日本人といった患者群に奏効例が多いという臨床的特徴であった[9, 18]．

その後2004年春，米国でEGFRの遺伝子変異がゲフィチニブの感受性と強い相関があることを示唆する報告がなされ，大いに注目された[20, 26]．その遺伝子変異は，EGFRのTK領域をコードしているexon18～24のうち，最初の4つのexonの遺伝子領域に起こり，特にexon19の欠失変異とexon21の点突然変異の頻度が高いことが示されている．

さらにこのEGFR遺伝子変異が非喫煙者，腺癌，女性，東洋人において高い頻度で認められ[17, 20, 26, 27]，先に見出されたゲフィチニブ奏効予測因子と相関し，それを支持するものであった．その遺伝子変異がゲフィチニブ感受性を強める機序としては，遺伝子変異をもったEGFRが，そのTKのATP結合部位に構造変化が生じる結果，EGFRが恒常的に活性化して悪性度が高まる一方，ゲフィチニブとの親和性が高まり，効腫瘍効果が高まると考えられている（**図2**）[10]．

この極めて重要な発見がなされた後，日本においてEGFR変異を有する未治療進行非小細胞肺癌に対する第2相臨床試験が行われ，約75％で腫瘍縮小効果が認められ[2, 14]，また肺癌術後再発の患者におけるゲフィチニブ治療患者の後ろ向き調査では，EGFR遺伝子変異患者群で生存期間の有意な延長が示された[23]．このように，EGFR-TK遺伝子変異は臨床における重要な感受性予測因子

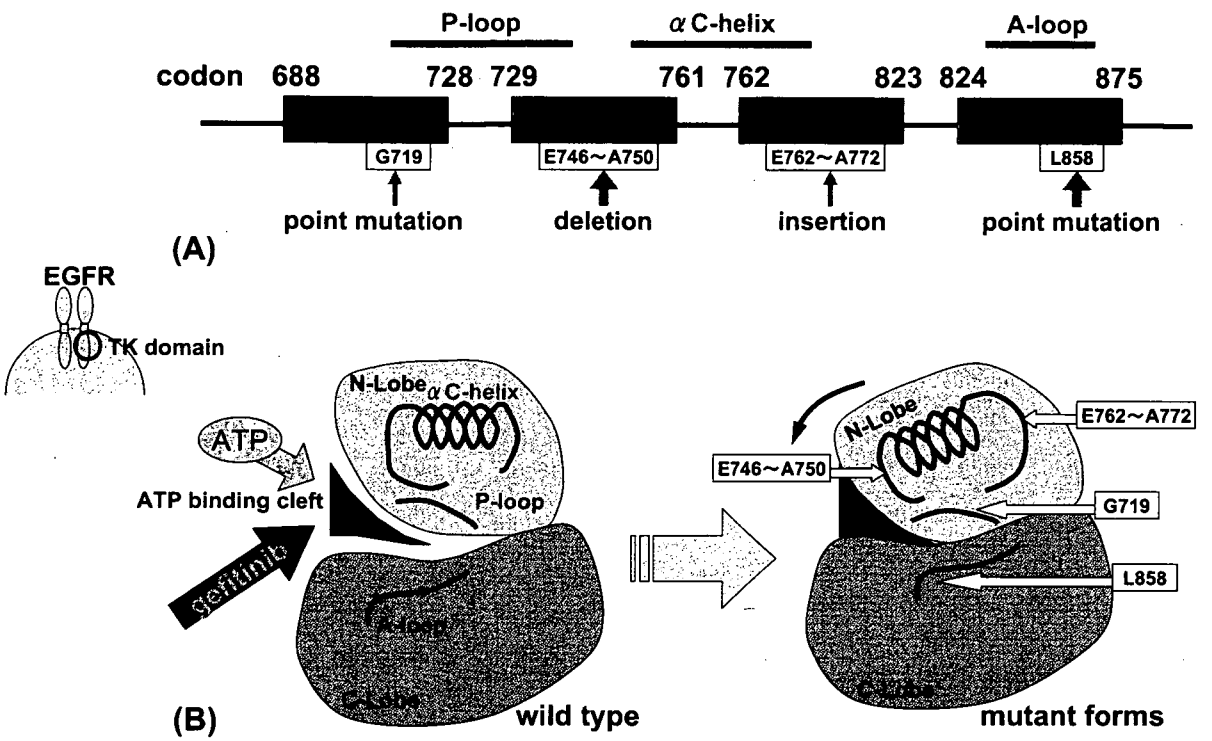


**図2　ゲフィチニブ感受性腫瘍細胞におけるEGFR遺伝子変異の部位，およびそれによるTKタンパクの立体構造の変化**（[10]を参考に作成）

EGFR-TK部位のタンパク構造は，2つの類球形のN-lobeとC-lobeから成り立っている（Bの左）．EGFR遺伝子変異は，この立体構造におけるN-lobeおよびC-lobeの一部に関係する最初の4つのexon内で起こる（A）．その結果，TKのタンパク立体構造がATP binding cleftを狭くする方向へ変化することで，EGFRが恒常的に活性化され悪性度が高まり，同時にゲフィチニブとの親和性が強くなり，抗腫瘍効果が高まると考えられている（Bの右）．

であることは間違いないと考えられている．ただし，それらが完全には一致せず，遺伝子変異がなくても感受性を示す例やその逆の例もわずかに存在することも付け加えておく．

その後，このEGFR遺伝子にさらに二次的な遺伝子変異が起こるとゲフィチニブに抵抗性をもたらすことが報告された[16, 28]．以上のように，臨床使用開始後，薬剤感受性と遺伝子変異との関係が詳細に研究され，明らかになってきたことはこの薬剤の特徴の一つであり，意義は大きい．

## V．ゲフィチニブの肺癌脳転移に対する効果

ゲフィチニブの臨床使用が開始になって以降，脳転移例での腫瘍縮小効果が世界中から報告されている（**図3**）．**表1**は，肺癌脳転移巣に対してのゲフィチニブ治療の効果についてのこれまでに報告されている主な調査である．

東洋からの報告が多いのは，前述のごとく東洋人であることが感受性因子の一つであり，ゲフィ

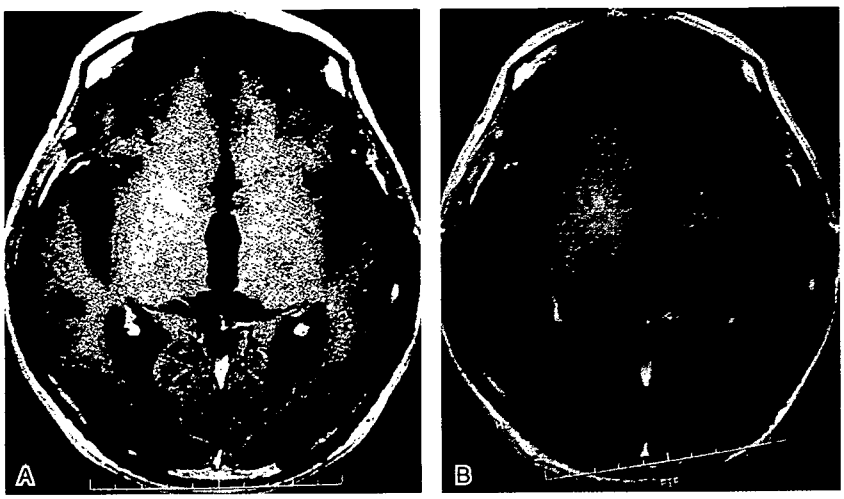


**図3　脳転移巣に対してゲフィチニブが効果を示した患者のMRI所見（61歳男性，肺腺癌原発）**
A：ゲフィチニブ治療直前のMRI．全脳放射線照射後に一旦縮小効果を示した後，最増大した右基底核病変を認める．
B：ゲフィチニブ治療開始後4ヵ月後のMRI．右基底核病変はほぼ消失している．

**表1　肺癌脳転移症例に対するゲフィチニブ治療の過去の報告例**

| 著者，発表年 | 調査法 | 国 | 患者数（男/女） | 腺癌（%） | 奏効率 | 効果期間（月）* |
|---|---|---|---|---|---|---|
| Ceresoliら[5],2004 | 前向き | 伊 | 41(29/12) | 23(56%) | 10% | 13.5 |
| Hottaら[13],2004 | 後ろ向き | 日本 | 14(7/7) | 12(86%) | 43% | 7.7 |
| Nambaら[24],2004 | 後ろ向き | 日本 | 15(9/6) | 11(73%) | 60% | 8.7 |
| Shimatoら[34],2005 | 後ろ向き | 日本 | 8(6/2) | 6(75%) | 63% | 12 |
| Chiuら[6],2005 | 前向き | 台湾 | 76(40/36) | 53(69.7%) | 33% | 5 |
| Leeら[19],2005 | 前向き | 韓国 | 10** (NA) | 10(100%) | 70% | NA |
| Wuら[36],2007 | 前向き | 中国 | 40(22/18) | 40(100%) | 32% | 9.0 |

NA: not available
*効果期間：median progression-free survival，あるいは median duration of response
**全登録患者37例中，脳転移合併の患者数のみ表示

チニブが東洋の国々を中心に承認されていることを反映していると思われる．イタリアからの報告では奏効率が10％と東洋からの報告に比べ低い数字となっており，脳転移巣でも東洋人でより効きやすいことが想像される．

韓国のLeeらの報告は，患者群を非喫煙者かつ進行腺癌に限り，ゲフィチニブを第一選択肢として治療している臨床試験で注目されるが，臨床的奏効因子を満たす患者が大部分を占め，極めて高い奏効率となっている[19]．したがって治療対象を，奏効因子を満たす患者群に限れば，肺癌での報告と同様に脳転移においてもかなり高い奏効率

が得られる可能性があると思われる．さらに，脳転移巣においてもEGFR-TK領域の遺伝子変異がゲフィチニブ感受性に強く相関すると考えられ，効果予測因子として重要である[34]．効果の持続期間をみてみると，中央値で1年以下の報告が多く，一旦は効果を示してもやがては効かなくなることは肺癌に対する効果と同様であり，効果には限界がある．

また，この薬剤の延命効果については肺癌でも議論のあるところであるが，脳転移巣に対しての延命効果についても今のところ評価できる調査は報告されていない．興味深い症例報告としては，肺病変と同時に多発性脳転移で発症後，ゲフィチニブ治療のみで2年以上の間，脳転移巣の進行なく良好な経過をたどった症例や[22]，馬尾症状等で発症した脳脊髄髄膜播種に対しゲフィチニブ治療を行い，2週間で完全に神経症状が消失した症例の報告等がある[31]．ゲフィチニブは，神経症状の著明な改善とそれに伴うADL向上，さらに生存期間の延長効果をもたらす可能性を秘め，大きな恩恵を受ける患者もいることは確かである．

以上のようにゲフィチニブによる劇的奏効例がある一方で，抵抗性の症例や初期は奏効しても急激に抵抗性となる症例があるのも特徴である．肺癌治療で初期にゲフィチニブが奏効後に抵抗性となる場合，脳転移あるいは髄膜播種として進展する頻度が高いという報告もあり[25]，ゲフィチニブ治療の終末像として脳転移が現れることがあることも事実である．

ゲフィチニブによる脳転移あるいは髄膜播種に対する効果には，同薬のBBB透過性や髄液移行性も大きくかかわると考えられる．ゲフィチニブのBBB透過性は確認されていないが，分子量の小さな薬剤であり，有効例のほとんどは肺癌での使用量と同じ一日量250mgで継続されていることから，同量で脳転移巣や髄液腔へ十分に浸透する可能性が考えられる．一方で，髄膜播種合併例で，ゲフィチニブの十分な髄液移行と効果出現までに一日量1,000mg以上まで増量を必要とした症例の報告もあり[15]，症例によっては至適投与量が異なる可能性も考えられる．

脳転移巣に対する現在の標準的治療は放射線治療であり，現時点ではゲフィチニブを積極的治療の方法として使用することは難しく，過度に期待をするべきではない．しかし，非小細胞肺癌の脳転移例で放射線治療が困難な場合，治療歴や全身的な病状を考慮したうえで，QOL改善を期待してゲフィチニブを使用するという選択肢があることも知っておくべきであろう．その際には，急性肺傷害等の有害事象の危険性を十分認識し，また有効性を予測するうえで，患者背景やEGFR-TK領域の遺伝子変異の有無を検討することは重要であり，呼吸器専門医との協力が必要である．

## Ⅵ．ゲフィチニブのグリオーマに対する治療の可能性

悪性グリオーマでもEGFR遺伝子過剰発現が高頻度で認められ，ゲフィチニブ治療の可能性が期待された．米国やイタリアではすでに再発悪性グリオーマ症例に対するゲフィチニブ治療の第2相臨床試験が行われ，腫瘍制御例はあったものの腫瘍縮小例はなく，6-month event free survivalが

13～14％，median overall survivalが24.6～39.4週と効果は限られたものであったと報告している[8,30]．これらの試験ではEGFRあるいは細胞外領域に関係する遺伝子変異であるEGFRvⅢの発現やEGFR遺伝子増幅等についても解析しているが，それらはゲフィチニブ効果とはまったく相関しなかった[30]．

その後，肺癌におけるEGFR-TK領域の遺伝子変異が発見されたのを受けグリオーマでも解析されているが，glioblastoma，anaplastic oligodendroglioma，low grade gliomaではそれらの遺伝子変異は認められず[3,21]，グリオーマにおけるEGFRの生物学的意義やその他の分子機序は肺癌におけるそれとは異なると考えられ，グリオーマではゲフィチニブによる効果を期待できない理由と考えられている．

2005年には，臨床試験の結果から，EGFRvⅢとPTEN両者の発現がゲフィチニブ感受性に強く相関すると報告され，グリオーマに対してゲフィチニブ治療を考える際は，EGFRとその下流のシグナル伝達系を含めた因子を考える必要があることを示している．そして，新しい試みとしては，ゲフィチニブに加えてEGFR経路下流のmTOR（mammalian target of rapamycin）の阻害剤を用いる試みもされており，一定の効果が得られたことが報告されている[7,29]．

このようにグリオーマにおいてはゲフィチニブ単剤での分子標的治療には限界があると考えられ，関連する他の分子を同時に狙い撃つような戦略が必要と考えられる．

## Ⅶ．おわりに

現在，脳転移に対しては放射線治療が中心となっているが，癌が全身疾患であることを考えれば脳を含めた全身的な効果を導いてくれる治療法が望まれる．これまでに報告されたゲフィチニブによる肺癌脳転移に対する効果は，脳転移に対する薬物治療の可能性を示してくれたと言える．今後は他の癌種も含め，脳転移巣への効果という視点からも抗腫瘍薬治療の研究が進められることを期待する．

ゲフィチニブの感受性と遺伝子変異との関連についての重要な発見は，薬物治療において「効く患者」をいかに選ぶかということの重要性を認識させられる．今後は，テーラーメイド治療の考え方が高まると考えられ，ゲフィチニブにおける成果は他の抗腫瘍薬治療の研究においても大いに参考となるであろう．

ゲフィチニブはまた，分子標的治療薬の可能性を示したと同時に，腫瘍生物学の見識を深めさらに問題点や課題も提示してくれたという点でも意味深い．他の分子標的治療を含め，今後のさらなる発展に期待し，注目していきたい．

### 文　献

1）Arteaga CL: Overview of epidermal growth factor receptor biology and its role as a therapeutic target in human neoplasia. Semin Oncol 29: 3-9, 2002
2）Asahina H, Yamazaki K, Kinoshita I, et al : A phase II trial of gefitinib as first-line therapy for advanced non-small cell lung cancer with epidermal growth factor receptor mutations. Br J Cancer 95: 998-1004, 2006
3）Barber TD, Vogelstein B, Kinzler KW, et al : Somatic mutations of EGFR in colorectal cancers and glioblastomas.

N Engl J Med 351: 2883, 2004
4) Cappuzzo F, Gregorc V, Rossi E, et al : Gefitinib in pretreated non-small-cell lung cancer (NSCLC) : analysis of efficacy and correlation with HER2 and epidermal growth factor receptor expression in locally advanced or metastatic NSCLC. J Clin Oncol 21: 2658-2663, 2003
5) Ceresoli GL, Cappuzzo F, Gregorc V, et al : Gefitinib in patients with brain metastases from non-small-cell lung cancer: a prospective trial. Ann Oncol 15: 1042-1047, 2004
6) Chiu CH, Tsai CM, Chen YM, et al : Gefitinib is active in patients with brain metastases from non-small cell lung cancer and response is related to skin toxicity. Lung Cancer 47: 129-138, 2005
7) Doherty L, Gigas DC, Kesari S, et al : Pilot study of the combination of EGFR and mTOR inhibitors in recurrent malignant gliomas. Neurology 67: 156-158, 2006
8) Franceschi E, Cavallo G, Lonardi S, et al : Gefitinib in patients with progressive high-grade gliomas: a multicentre phase II study by Gruppo Italiano Cooperativo di Neuro-Oncologia (GICNO) . Br J Cancer 96: 1047-1051, 2007
9) Fukuoka M, Yano S, Giaccone G, et al : Multi-institutional randomized phase II trial of gefitinib for previously treated patients with advanced non-small-cell lung cancer. J Clin Oncol 21: 2237-2246, 2003
10) Gazdar AF, Shigematsu H, Herz J, et al : Mutations and addiction to EGFR: the Achilles 'heal' of lung cancers ? Trends Mol Med 10: 481-486, 2004
11) Giaccone G, Herbst RS, Manegold C, et al : Gefitinib in combination with gemcitabine and cisplatin in advanced non-small-cell lung cancer: a phase III trial--INTACT 1. J Clin Oncol 22: 777-784, 2004
12) Herbst RS, Giaccone G, Schiller JH, et al : Gefitinib in combination with paclitaxel and carboplatin in advanced non-small-cell lung cancer: a phase III trial--INTACT 2. J Clin Oncol 22: 785-794, 2004
13) Hotta K, Kiura K, Ueoka H, et al : Effect of gefitinib ('Iressa', ZD1839) on brain metastases in patients with advanced non-small-cell lung cancer. Lung Cancer 46: 255-261, 2004
14) Inoue A, Suzuki T, Fukuhara T, et al : Prospective phase II study of gefitinib for chemotherapy-naive patients with advanced non-small-cell lung cancer with epidermal growth factor receptor gene mutations. J Clin Oncol 24: 3340-3346, 2006
15) Jackman DM, Holmes AJ, Lindeman N, et al : Response and resistance in a non-small-cell lung cancer patient with an epidermal growth factor receptor mutation and leptomeningeal metastases treated with high-dose gefitinib. J Clin Oncol 24: 4517-4520, 2006
16) Kobayashi S, Boggon TJ, Dayaram T, et al : EGFR mutation and resistance of non-small-cell lung cancer to gefitinib. N Engl J Med 352: 786-792, 2005
17) Kosaka T, Yatabe Y, Endoh H, et al : Mutations of the epidermal growth factor receptor gene in lung cancer: biological and clinical implications. Cancer Res 64: 8919-8923, 2004
18) Kris MG, Natale RB, Herbst RS, et al : Efficacy of gefitinib, an inhibitor of the epidermal growth factor receptor tyrosine kinase, in symptomatic patients with non-small cell lung cancer: a randomized trial. JAMA 290: 2149-2158, 2003
19) Lee DH, Han JY, Lee HG, et al : Gefitinib as a first-line therapy of advanced or metastatic adenocarcinoma of the lung in never-smokers. Clin Cancer Res 11: 3032-3037, 2005
20) Lynch TJ, Bell DW, Sordella R, et al : Activating mutations in the epidermal growth factor receptor underlying responsiveness of non-small-cell lung cancer to gefitinib. N Engl J Med 350: 2129-2139, 2004
21) Marie Y, Carpentier AF, Omuro AM, et al : EGFR tyrosine kinase domain mutations in human gliomas. Neurology 64: 1444-1445, 2005
22) Matsuyama W, Yamamoto M, Machida K, et al : [Two lung adenocarcinoma patients with multiple brain metastasis treated with Gefitinib and surviving more than 2 years] Nihon Kokyuki Gakkai Zasshi 44: 653-658, 2006
23) Mitsudomi T, Kosaka T, Endoh H, et al : Mutations of the epidermal growth factor receptor gene predict prolonged survival after gefitinib treatment in patients with non-small-cell lung cancer with postoperative recurrence. J Clin Oncol 23: 2513-2520, 2005
24) Namba Y, Kijima T, Yokota S, et al : Gefitinib in patients with brain metastases from non-small-cell lung cancer: review of 15 clinical cases. Clin Lung Cancer 6: 123-128, 2004
25) Omuro AM, Kris MG, Miller VA, et al : High incidence of disease recurrence in the brain and leptomeninges in patients with nonsmall cell lung carcinoma after response to gefitinib. Cancer 103: 2344-2348, 2005
26) Paez JG, Janne PA, Lee JC, et al : EGFR mutations in lung cancer: correlation with clinical response to gefitinib therapy. Science 304: 1497-1500, 2004
27) Pao W, Miller V, Zakowski M, et al : EGF receptor gene mutations are common in lung cancers from " never smokers" and are associated with sensitivity of tumors to gefitinib and erlotinib. Proc Natl Acad Sci U S A 101: 13306-13311, 2004
28) Pao W, Miller VA, Politi KA, et al : Acquired resistance of

lung adenocarcinomas to gefitinib or erlotinib is associated with a second mutation in the EGFR kinase domain. PLoS Med 2: e73, 2005
29) Reardon DA, Quinn JA, Vredenburgh JJ, et al : Phase 1 trial of gefitinib plus sirolimus in adults with recurrent malignant glioma. Clin Cancer Res 12: 860-868, 2006
30) Rich JN, Reardon DA, Peery T, et al : Phase II trial of gefitinib in recurrent glioblastoma. J Clin Oncol 22: 133-142, 2004
31) Sakai M, Ishikawa S, Ito H, et al : Carcinomatous meningitis from non-small-cell lung cancer responding to gefitinib. Int J Clin Oncol 11: 243-245, 2006
32) Schuette W: Treatment of brain metastases from lung cancer: chemotherapy. Lung Cancer 45 Suppl 2: S253-S257, 2004
33) Selvaggi G, Novello S, Torri V, et al : Epidermal growth factor receptor overexpression correlates with a poor prognosis in completely resected non-small-cell lung cancer. Ann Oncol 15: 28-32, 2004
34) Shimato S, Mitsudomi T, Kosaka T, et al : EGFR mutations in patients with brain metastases from lung cancer: association with the efficacy of gefitinib. Neuro oncol 8: 137-144, 2006
35) Thatcher N, Chang A, Parikh P, et al : Gefitinib plus best supportive care in previously treated patients with refractory advanced non-small-cell lung cancer: results from a randomised, placebo-controlled, multicentre study (Iressa Survival Evaluation in Lung Cancer) . Lancet 366: 1527-1537, 2005
36) Wu C, Li YL, Wang ZM, et al : Gefitinib as palliative therapy for lung adenocarcinoma metastatic to the brain. Lung Cancer. 2007 Apr : 12, 2007
37) 日本肺癌学会ゲフィチニブ使用に関するガイドライン作成委員会. ゲフィチニブ使用に関するガイドライン: 日本肺癌学会ホームページ
＜http://www.haigan.gr.jp/gefiti-gaid.pdf＞

J Neurooncol
DOI 10.1007/s11060-007-9338-y

CLINICAL STUDY—PATIENT STUDIES

# Stereotactic radiosurgery for atypical and anaplastic meningiomas

**Hideyuki Kano · Jun A. Takahashi · Takahisa Katsuki · Norio Araki · Natsuo Oya · Masahiro Hiraoka · Nobuo Hashimoto**

Received: 1 December 2006 / Accepted: 18 January 2007


**Abstract** Atypical and anaplastic meningiomas frequently recur in the relatively short-term after surgery. We have followed such postoperative cases by short-interval repeated MRI and have performed stereotactic radiosurgery (SRS) for progressive tumors as a salvage therapy. The objective of this report was assessment of the degree of tumor control, the risk of complications, and the presence of variables that predict outcome in patients treated with SRS for high-grade meningiomas. We reviewed 12 high-grade meningioma patients with 30 lesions treated by Linac-based SRS at Kyoto University Hospital between 1997 and 2002. They included 10 atypical meningiomas and 2 anaplastic ones according to the WHO classification. A mean tumor volume was 4.40cc and a mean marginal dose of SRS was 18.0 Gy (12–20 Gy). After a mean follow-up period of 43.4 months (6–84 months), 13 lesions had progression tumor within the SRS field and 6 lesions had out of the SRS field. Nine of 14 lesions, which were treated by SRS with a marginal dose of less than 20 Gy, had local recurrence in the SRS field. In contrast, four of 16 lesions, which were treated with marginal dose of 20 Gy, had local recurrence in the SRS field. The marginal dose <20 Gy was a statistically significant factor for a short-term progression in high-grade meningiomas ($P = 0.0139$). Five-year progression-free survival ratio in lesions treated with SRS below 20 Gy and 20 Gy were 29.4% and 63.1%, respectively. In conclusion, based on our findings, we suggest that recurrent high-grade meningiomas be treated by SRS with a marginal dose exceeding 20 Gy.

**Keywords** Stereotactic radiosurgery · Meningioma · Atypical · Anaplastic

J. A. Takahashi (✉) · T. Katsuki · N. Hashimoto
Department of Neurosurgery, Kyoto University Faculty of Medicine, 54 Shyogoin-Kawaharacho, Sakyouku, Kyoto, Japan
e-mail: jat@kuhp.kyoto-u.ac.jp

H. Kano
Department of Neurosurgery, Kishiwada City Hospital, Osaka, Japan

N. Araki · M. Hiraoka
Department of Radiation Oncology, Kyoto University Faculty of Medicine, Kyoto, Japan

N. Oya
Department of Radiation Oncology, Graduate School of Medical Sciences, Kumamoto University, Kumamoto, Japan

## Introduction

Meningiomas arise from the dural covering of the brain. They account for 13–26% of all primary intracranial tumors and are the most common benign intracranial neoplasms. Histologically, 4–7% of meningiomas are atypical and 1–2% are anaplastic [1] and surgery has been the primary treatment modality regardless of subtype [2]. The extent of surgery plays an important role in predicting the risk of recurrence and may determine the need for adjuvant therapy [3–5]. In selected patients, stereotactic radiosurgery (SRS) is an effective treatment for benign meningiomas both as an adjunct to subtotal resection and as the primary therapy [6–10]. Benign meningiomas have an indolent natural history and an excellent cure rate with either surgery or radiotherapy [11]. On the other hand, atypical and anaplastic meningiomas tend to recur in the relatively short term even after radical surgical

resection. The 5-year survival rate for these histologically aggressive tumors is reportedly 50–70% [11, 12]. We closely followed operated patients with high-grade meningiomas by MRI studies and performed SRS as salvage therapy in patients with tumor progression. Here we report the degree of tumor control, the risk of complications, and the variables that predict treatment outcomes in SRS-treated patients with high-grade meningiomas.

## Methods and materials

Between October 1997 and November 2002, 12 patients with atypical or anaplastic meningioma underwent SRS at Kyoto University Hospital. Patients with hemangiopericytoma or neurofibromatosis-type 2 were excluded from this analysis. All included patients had histologically confirmed atypical or anaplastic meningioma diagnosed at the time of their initial craniotomy. There were 8 males and 4 females; their mean age was 58.5 years. All patients provided prior informed consent for inclusion in this study and the investigation was approved the by Ethics Committee of Kyoto University.

According to the 2000 WHO classification, the diagnosis of atypical meningioma is based on a combination of histological features, i.e. increased mitotic activity (4 or more mitoses per 10 high-power fields), hypercellularity, eosinophilic macronucleoli, sheetlike growth, and small cell collections [1, 13]. The diagnosis of anaplastic meningioma is based on the histological features of frank malignancy. These include "carcinoma-like" foci and/or highly mitotically active tumor cells with 10–20 or more mitoses per high-powered field, and far exceed the abnormalities present in atypical meningioma. We reviewed the histopathology of the 30 tumors included in this study; the diagnosis of atypical (WHO grade II) or anaplastic (WHO grade III) meningioma was confirmed by a neuropathologist [7].

In this series, 10 patients (83.3%) had atypical- and 2 (16.7%) had anaplastic meningiomas; all were treated with LINAC-based SRS using 6 MV X-ray beams generated by Clinac-2300c linear accelerator (Varian Inc., Palo Alto, CA) at Kyoto University Hospital. Treatment planning was carried out using the X-knife system (Radionics Inc., Burlington, MA), following a 3 mm-slice contrast-enhanced tumor lesions and critical structures, such as eyes, brain stem and optic nerves, were delineated. The characteristics of the 12 patients with 30 lesions are outlined in Table 1.

As 8 patients harbored 1- and 4 had 2 or more tumors, and 4 patients had undergone 2 or more SRS treatments, a total of 30 tumors were treated in the 12 patients. In 11 patients the tumors recurred after one or more operations, one patient underwent SRS as a primary treatment for late recurrence after surgical resection and 2 patients received external beam radiation therapy after microsurgery and before SRS.

**Table 1** Summary of 12 meningioma patients treated by SRS and characteristics of their 30 lesions

| Characteristics | Mean/median | Range |
|---|---|---|
| *Patients (n = 12)* | | |
| Age (yrs) | 58.5 / 63 | 32–69 |
| Sex | | |
| Male | 8 | |
| Female | 4 | |
| *Tumors (n = 30)* | | |
| Location | | |
| Skull base | 6 | |
| Non-skull base | 24 | |
| Grade | | |
| Atypical | 25 | |
| Anaplastic | 5 | |
| Target volume ($cm^3$) | 4.40/2.87 | 0.29–18 |
| Follow-up period (months) | 43.4/44 | 6–84 |
| Marginal dose (Gy) | 18/19 | 12–20 |
| 80% dose-coverage volume (%) | 97.1/98.5 | 80–100 |
| Prescription dose | | |
| <20Gy | 14 | |
| 20Gy | 16 | |

Medical records were reviewed for data such as age and sex and the dates of meningioma diagnosis, completion of radiotherapy, and death or most recent follow-up.

A neurosurgeon, radiation oncologist, and radiation physicist participated in all dosimetry planning. The highest emphasis was placed on designing an isodose line that conformed to the exact tumor shape. The mean radiation dose to the periphery of the lesion was 18.0 Gy (range 12–20 Gy); in most cases delivery was to the 80% isodose line (range 80–100%). All patients were treated with a single isocenter; the collimator diameter ranged from 12.5 to 35 mm. In cases with an irregular target, the treatment plan was modified by changing the weight, plane and angle of the arcs to achieve higher dose conformity.

The radiographs were visually inspected by a radiologist to monitor changes in tumor size over time. Pre- and post-treatment images were available for comparison studies in all patients. Tumor dimensions were compared in the axial, sagittal, and coronal planes. A decrease in any one dimension without a concomitant increase in any other dimension was recorded as a decrease in tumor size, growth in any plane as an increase. The tumor size was recorded as unchanged, decreased, or increased at each point of

inspection. Tumor growth adjacent to the irradiated tumor and outside the isodose volume was defined as margin recurrence; tumors that developed at noncontiguous sites were considered distant recurrences.

For statistical analysis we constructed Kaplan–Meier plots for survival and progression-free survival (PFS) using the dates of diagnosis, first surgery, first SRS, follow-up scans, and death or last follow-up. PFS and overall survival time were calculated from the day of the first SRS using the Kaplan–Meier method. Univariate analysis was performed on the Kaplan–Meier curves using the logrank statistic with $P < 0.05$ set as significant [14]. Standard statistical processing software (SPSS, version 14.0J and Prism, version 4.0) was used.

## Results

Of the 12 patients, 11 reported for regular postoperative clinical visits. One patient manifested tumor progression 4 months after undergoing SRS; she underwent surgical resection 17 months from the date of SRS and the diagnosis of atypical meningioma was verified histologically.

The patients were observed for a mean of 43.4 months (range 6–84 months); at the end of the observation period 10 patients were alive. Death in one case was the result of lung metastasis from anaplastic meningioma which was based on the histological features, the other patient died from disease progression. The overall 5-year survival rate was 80.8% (Fig. 1). We treated 14 lesions with a lower radiation dose than 20 Gy to avoid severe anticipated toxicity. Six lesions were in close proximity to the brainstem or optic nerve (to optic nerve, <8 Gy). Two pairs of dual lesions treated simultaneously were close to each other, and 2 lesions were near prior radiosurgery sites. One lesion was located within the high dose volume of a prior EBRT field. One lesion that was treated as a low-grade meningioma was determined to be an atypical meningioma at the time of salvage surgery following progression after SRS. The other 16 lesions were treated by SRS with a marginal dose of 20 Gy. The statistics for PFS at 20 Gy and <20 Gy are shown in Fig. 2; the 2- and 5-year PFS rate for the 12 patients with high-grade meningioma was 48.3%. The median and mean time to recurrence was 4 and 7.7 months, respectively (range 3–23 months); 6 of the 12 patients (13 of 30 lesions) manifested in-field recurrence.

We performed Univariate analysis using the logrank test to assess factors that influence the length of PFS. The variables were sex, age (older or younger than 50 years), tumor location (skull base or non-skull base), target volume (more or <8 cc, and more or <2.87 cc), dose (20 Gy or <20 Gy), and tumor grade (atypical or anaplastic). As shown in Table 2, 9 of 14 (64.3%) lesions treated by SRS with a marginal dose below 20 Gy recurred in the radiation field; the median time to progression (TTP) was 6 months. In contrast, 4 of 16 (25.0%) lesions treated with a marginal dose of 20 Gy exhibited a local recurrence in the radiation field; the median TTP was 21 months. The radiation dose (20 Gy) was the only factor significantly associated with better PFS.

Kaplan–Meier plots, generated for overall survival and PFS (Figs. 1, 2) showed that patients treated with doses below 20 Gy had a 1-, 2-, and 5-year PFS of 39.2, 29.4 and 29.4%, respectively. Patients who had received 20 Gy had a 1-, 2-, and 5-year PFS of 85.2%, 63.1%, and 63.1%, respectively ($P = 0.0139$). The characteristics of lesions treated with 20 Gy or <20 Gy

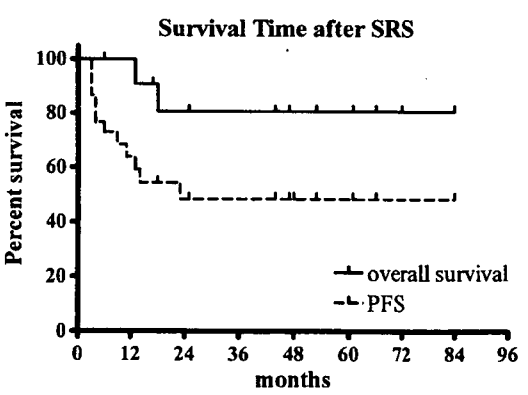


**Fig. 1** Kaplan–Meier estimate of overall survival curve and progression-free survival curve in all patients after the first SRS for high-grade meningiomas

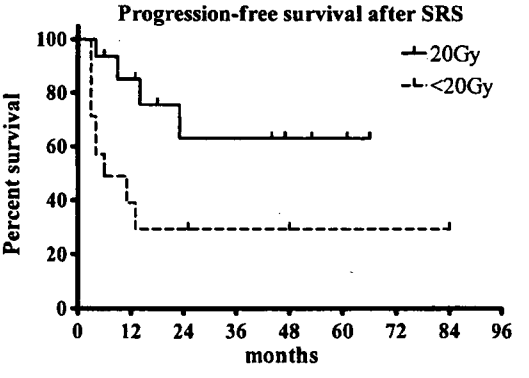


**Fig. 2** Kaplan–Meier progression-free survival curves in all patients after the first SRS for high-grade meningiomas treated with SRS doses of 20 Gy or <20 Gy. The delivery of 20 Gy was a statistically significant factor for longer progression-free survival ($P = 0.0139$)

**Table 2** Characteristics of lesions treated by SRS with 20 Gy or <20Gy

| Marginal dose | (<20Gy) | (20Gy) |
|---|---|---|
| Mean age | 59.9 years | 50 years |
| Mean/median target volume | 4.10/1.75 $cm^3$ | 4.67/2.91 $cm^3$ |
| Mean/median marginal dose | 15.2/15 Gy | 20/20 Gy |
| 80% dose coverage volume | 98.9% | 98.4% |
| Total lesions | 14 | 16 |
| Recurrent lesions | 9 | 4 |
| 1-year PFS rates | 39.2% | 85.2% |
| 2-year PFS rates | 29.4% | 63.1% |
| 5-year PFS rates | 29.4% | 63.1% |

are shown in Table 2. The median and mean volume of all tumors was 2.87 cc and 4.40 cc, respectively (range, 0.29–18 cc). The mean and median tumor volume of lesions treated with less than 20 Gy was 4.10 cc and 1.75 cc, respectively. The mean and median tumor volume of lesions treated with 20 Gy was 4.67 cc and 2.91 cc, respectively. The mean and median dose of lesions treated with <20 Gy was 15.2 Gy and 15 Gy, respectively. PFS was not affected by the tumor size; the 80% dose coverage volume was 98.9% at <20 Gy and 98.4% at 20 Gy (Table 2). In the cases of atypical meningioma (25 lesions), Kaplan–Meier plots, generated for overall survival and PFS showed that patients (12 lesions) treated with doses below 20 Gy had a 5-year PFS of 29.4%. Patients (13 lesions) who had received 20 Gy had a 5-year PFS of 63.1% ($P = 0.0213$). There were 2 anaplastic meningiomas with 5 lesions. One lesion recurred in 23 months after SRS. The mean follow-up period was 26.5 months. The overall survival rate was 100%, and a 3-year PFS rate was 50% (median PFS, 35 months).

Two (17%) of the 12 patients treated with SRS developed radiation toxicity. They had received doses of 17.6 Gy and 20 Gy. Asymptomatic perifocal edema from radiation-induced angiopathy occurred at 41 months post-SRS treatment in one patient and after 61 months in the other.

## Discussion

The results of this study indicate that SRS with a marginal dose of 20 Gy may help to prolong PFS in patients with high-grade meningiomas.

### External-beam radiotherapy (EBRT) for high-grade meningiomas

Atypical and anaplastic meningiomas have higher local recurrence- and lower survival rates than benign meningiomas. In the past, the initial treatment for anaplastic meningiomas was surgical removal followed by conventional EBRT. Studies on the clinical course of completely- or partially resected atypical and anaplastic meningiomas with or without additional adjuvant EBRT reported 5-year PFS rates between 32 and 48%, and 5-year overall survival rates between 28 and 95% [11, 15–18]. Goldsmith et al. [15] found that patients with anaplastic meningioma had significantly less favorable outcomes than did patients with tumors of a benign histology; their 5-year overall survival- and PFS rate was 58% and 48%, respectively. These data show that EBRT alone is not sufficient to treat high-grade meningiomas.

### SRS for high-grade meningiomas

Stereotactic radiosurgery is now considered an option for the treatment of primary or recurrent meningiomas. It proved useful for benign meningiomas and excellent control rates were obtained when SRS was used as an adjunct to surgical tumor removal. However, as shown in Table 3 [10, 19–22], the effectiveness of SRS in patients with atypical and anaplastic meningioma remained to be elucidated.

Stafford et al. [10] reported that the cause-specific 5-year survival rate for SRS-treated patients with benign, atypical, and anaplastic meningioma was 100,

**Table 3** SRS for atypical and anaplastic meningiomas

| Authors | Year | Histology | Patients (lesions) | F/U | Marginal dose | 5-year-PFS ratio | 5-year-survival ratio |
|---|---|---|---|---|---|---|---|
| Hakim | 1998 | Atypical | 26 | 31 M | 15 Gy | N.A. | 83% (4 year) |
| | | Malignant | 18 | | | | 22% (4 year) |
| Ojemann | 2000 | Malignant | 22 (26) | 29 M | 16 Gy | 26% | 40% |
| Stafford | 2001 | Atypical | 13 | 40 M | 16 Gy | 68% | 76% |
| | | Malignant | 9 | | | 0% | 0% |
| Harris | 2003 | Atypical | 18 | 27.6 M | 14.9 Gy | 83% | 59% |
| | | Malignant | 12 | | 15.7 Gy | 72% | 59% |
| Huffmann | 2005 | Atypical | 15 (21) | 35 M | 14–18 Gy | 1 recurrent | N.A. |
| Kano | 2006 | High-grade | 7 (14) | 43.4 M | <20 Gy | 29.4% | 80.8% |
| | | | 7 (16) | | 20 Gy | 63.1% | |

F/U, follow-up periods; PFS, progression-free survival; N.A., not available

76, and 0%, respectively ($P < 0.0001$); the 5-year local control rate was 89%. PFS rates were correlated with the histological features of the tumors ($P < 0.0001$); patients with benign tumors had a 5-year PFS rate of 93%; in patients with atypical or anaplastic meningiomas this rate was 68 and 0%, respectively. They also found that SRS-treated patients with high-grade meningiomas manifested high recurrence rates, and that despite aggressive treatment that included surgery, conventional EBRT, and SRS, these patients continued to exhibit lower cause-specific survival rates.

Ojemann et al. [22] who treated 22 anaplastic meningioma patients with gamma knife radiosurgery as boost to conventional EBRT over an 8-year period reported a 5-year overall survival rate of 40%. The 5-year PFS rate was 26%. In their series, age (<50 years) and tumor volume (<8 cc) were significant predictors of time to progression and length of survival. In addition, the 2-year survival rate of patients treated with doses below 15 Gy was 75%; there were no 5-year survivors. On the other hand, patients treated with doses >15 Gy had 2- and 5-year survival rates of 69% and 50%, respectively ($P = 0.13$ by univariate, $P = 0.14$ by multivariate analysis). Nineteen of 22 patients experienced progression, despite receiving conventional EBRT (median dose, 55 Gy) 4.5 years earlier. In our series, the PFS rates were longer than in previously reported studies and we posit that the PFS prolongation is attributable to the delivery of a higher radiation dose.

The median and mean tumor volume in our 12 patients were 2.87 cc and 4.40 cc, respectively (range 0.29–18 cc) and thus smaller than in previously reported studies; only 5 tumors exceeded 8 cc. Three of 14 lesions treated for tumor volumes exceeding 2.87 cc exhibited local recurrence in the radiation field. And 10 of 16 lesions treated for tumor volumes <2.87 cc recurred in the radiation field. However, the tumor size had no significant effect on PFS.

Modha et al. [23] stated SRS has now become part of the armamentarium when treating high-grade meningiomas. It could probably be offered to the patient as soon as possible postoperatively for any nodular residual tumor, along with conventional EBRT to the tumor bed. Certainly, the invasive nature of these tumors has to be considered, and SRS may not have any effect on infiltrative areas not appreciated during treatment planning. Its role after complete resection of a high-grade meningioma is also less clear. Instead, conventional EBRT to the tumor bed should be administered. Huffman et al. [21] proposed early SRS for incompletely resected residual high-grade meningiomas. For gross totally resected tumors, conventional EBRT should be considered. If focal recurrences develop after resection or margin or distant recurrent high-grade meningiomas develop after radiosurgery, SRS is an alternative to repeated microsurgery. In our series, 2 patients received EBRT after operation and before SRS. Ten patients did not receive EBRT before SRS. Only 1 lesion recurred in the EBRT field. Excepting this lesion, we performed Univariate analysis using logrank test, a marginal dose of 20 Gy was a statistically significant factor for longer PFS ($P = 0.0173$).

High-grade meningiomas are not highly sensitive to conventional EBRT and even SRS fails to inhibit tumor growth for a prolonged period. As the marginal dose delivered to previously reported tumors (between 14 and 18 Gy) failed to achieve adequate tumor control, where possible, we increased it to 20 Gy. In patients with tumors near critical organs and in those who had undergone previous irradiation therapy, and in cases of the tumors of the close proximity to each other, to avoid creating of hotspots in the normal brain tissue, we had to restrict the marginal dose to 14–18 Gy. The dose coverage volume was over 95% for all lesions. Although our study population is relatively small, the 2- and 5-year PFS rate was 48.3%. The 5-year PFS of patients treated with 20 Gy was 63.1% compared to 29.4% in those who received <20 Gy ($P = 0.0139$). Since there was no significant difference in tumor volume between both groups, the extension of PFS had been contributed by higher marginal dose (Table 2). The latter had a median PFS of 6 months and significantly earlier in-field tumor recurrence. Based on our observations and the results of earlier studies that showed that the progression of low-grade meningiomas can be controlled with relatively low doses (15–18 Gy), we conclude that in patients with high-grade meningiomas, SRS should deliver a marginal dose exceeding 20 Gy.

Huffmann et al. [21] who treated 21 lesions by SRS at doses ranging from 14 to 18 Gy reported only one instance of in-field recurrence. Their patient with a local relapse was treated with an SRS dose of 15 Gy. In our series, a marginal dose exceeding 20 Gy was the only statistically significant factor for longer PFS in patients with high-grade meningiomas ($P = 0.0139$). According to Harris et al., [20] the aggressive use of early boost-SRS after craniotomy and conventional EBRT is an important adjuvant management strategy for residual or recurrent high-grade meningiomas. In patients with no disease progression and in those with smaller tumor volumes, there was a statistically significant correlation between early SRS delivered soon after craniotomy and better survival rates. Their

findings support our hypothesis that early SRS with a marginal dose exceeding 20 Gy contributes to the prolongation of PFS in patients with high-grade meningiomas.

In the present retrospective analysis, dose reduction was shown to be significantly associated with the shorter PFS. The limitation of this study was the exsistence of the considerable bias between the lower dose group and the higher dose group, especially in the tumor location, because the prescribed dose was reduced, in most cases, to avoid the location-specific toxicity. Nevertheless, the radiation dose in SRS seemed to be one of the substantial factors in control of high-grade meningiomas, considering that the radiobiological characteristic of the tumor was unlikely to depend on the tumor location.

## Complications

Shaw et al. [24, 25] reported the findings of a multicenter trial in which escalating doses were delivered to recurrent, previously irradiated primary and metastatic tumors until unacceptable central nervous system (CNS) toxicity was reached. Variables significantly related to toxicity were a tumor diameter >21 mm, higher Karnofsky performance status scores, and a higher tumor dose. The maximum tolerated SRS doses in their study population were 24 Gy, 18 Gy, and 15 Gy for tumors </= 20 mm, 21–30 mm, and 31–40 mm in maximum diameter. Unacceptable CNS toxicity, defined as irreversible severe neurological symptoms, clinically, radiographically, or histologically verified radiation necrosis, or death, was more likely to occur in patients with larger tumors. On the other hand, local tumor control depended primarily on the type of the recurrent tumor and the treatment unit. In our study, the tumor volume and SRS dose were not significantly related to toxicity. We delivered 20 Gy to 14 lesions; 2 patients treated with doses of 17.6 Gy and 20 Gy developed asymptomatic radiation necrosis.

In conclusions, based on our findings, we suggest that recurrent high-grade meningiomas be treated by SRS with a marginal dose exceeding 20 Gy. Because of the rarity of these tumors, a multicenter trial would be required to evaluate these issues in a prospective study.

**Acknowledgements** The authors thank Mrs. Ursula Petralia and Mr. BJS Aldrich for critical reading of the manuscript.

## References

1. Louis DN, Scheithauer BW, Budka H, von Deimlig A, Kepes JJ (2000) Pathology and genetics of tumours of the nervous system; World Health Organisation Classification of Tumours. Lyon: IARC Press, 176–184
2. Mirimanoff RO, Dosoretz DE, Linggood RM, Ojemann RG, Martuza RL (1985) Meningioma: analysis of recurrence and progression following neurosurgical resection. J Neurosurg 62:18–24
3. Condra KS, Buatti JM, Mendenhall WM, Friedman WA, Marcus RB Jr, Rhoton AL (1997) Benign meningiomas: primary treatment selection affects survival. Int J Radiat Oncol Biol Phys 39:427–436
4. Hoffmann W, Muhleisen H, Hess CF, Kortmann RD, Schmidt B, Grote EH, Bamberg M (1995) Atypical and anaplastic meningiomas—Does the new WHO-classification of brain tumours affect the indication for postoperative irradiation? Acta Neurochir (Wien) 135:171–178
5. Taylor BW Jr, Marcus RB Jr, Friedman WA, Ballinger WE Jr, Million RR (1988) The meningioma controversy: Postoperative radiation therapy. Int J Radiat Oncol Biol Phys 15:299–304
6. Engenhart R, Kimmig BN, Hover KH, Wowra B, Sturn V, van Kaick G, Wannenmacher M (1990) Stereotactic single high dose radiation therapy of benign intracranial meningiomas. Int J Radiat Oncol Biol Phys 19:1021–6
7. Kondziolka D, Flickinger JC, Perez B (1998) Judicious resection and/or radiosurgery for parasagittal meningiomas: Outcomes from a multicenter review. Gamma Knife Meningioma Study Group. Neurosurg 43:405–413
8. Kondziolka D, Levy EI, Niranjan A, Flickinger JC, Lunsford LD (1999) Long-term outcomes after meningioma radiosurgery: physician and patient perspectives. J Neurosurg 91:44–50
9. Jaaskelainen J, Haltia M, Servo A (1986) Atypical and anaplastic meningiomas: radiology, surgery, radiotherapy, and outcome. Surg Neurol 25:233–242
10. Stafford SL, Pollock BE, Foote RL, Link MJ, Gordon DA, Schomberg PJ, Leavitt JA (2001) Meningioma radiosurgery: tumor control, outcomes, and complications among 190 patients. Neurosurg 49(5):1029–1038
11. Palma L, Celli P, Franco C, Cantore G (1997) Long-term prognosis for atypical and malignant meningiomas: a study of 71 surgical cases. J Neurosurg 86:793–800
12. Kondziolka D, Lunsford LD, Coffey RJ, Flickinger JC (1991) Gamma knife radiosurgery of meningiomas. Stereotact Funct Neurosurg 57:11–21
13. Perry A, Scheithauer BW, Stafford SL, Lohse CM, Wollan PC (1999) "Malignancy" in meningiomas: a clinicopathologic study of 116 patients. Cancer 85:2046–2056
14. Kaplan EL, Meier P (1958) Nonparametric estimation from incomplete observations. J Am Stat Assoc. 53:457–481
15. Goldsmith BJ, Wara WM, Wilson CB, Larson DA (1994) Postoperative irradiation for subtotally resected meningiomas. A retrospective analysis of 140 patients treated from 1967 to 1990. J Neurosurg 80:195–201
16. Goyal LK, Suh JH, Mohan DS, Prayson RA, Lee J, Barnett GH (2000) Local control and overall survival in atypical meningioma: a retrospective study. Int J Radiat Oncol Biol Phys 46:57–61
17. Ojemann SG, Sneed PK, Larson DA, Gutin PH, Berger MS, Verhey L, Smith V, Petti P, Wara W, Park E, McDermott MW (2000) Radiosurgery for malignant meningioma: results in 22 patients. J Neurosurg 93(Suppl 3):62–67
18. Milosevic MF, Frost PJ, Laperriere NJ, Wong CS, Simpson WJ (1996) Radiotherapy for atypical or malignant intracranial meningioma. Int J Radiat Oncol Biol Phys 34:817–822
19. Hakim R, Alexander E III, Loeffler JS, Shrieve DC, Wen P, Fallon MP, Stieg PE, Black PM (1998) Results of linear

accelerator-based radiosurgery for intracranial meningiomas. Neurosurg 42:446–453
20. Harris AE, Lee JY, Omalu B, Flickinger JC, Kondziolka D, Lunsford LD (2003) The effect of radiosurgery during management of aggressive meningiomas. Surg Neurol 60:298–305
21. Huffmann BC, Reinacher PC, Gilsabach JM (2005) Gamma knife surgery for atypical meningiomas. J Neurosurg 102(Suppl):283–286
22. Katz TS, Amdur RJ, Yachnis AT, Mendenhall WM, Morris CG (2005) Pushing the limits of radiotherapy for atypical and malignant meningioma. Am J Clin Oncol 28:70–74
23. Modha A, Gutin HP. (2005) Diagnosis and treatment of atypical and anaplastic meningiomas: a review. Neurosurgery 57:538–550
24. Shaw E, Scott C, Souhami L, Dinapoli R, Bahary JP, Kline R, Wharam M, Schultz C, Davey P, Loeffler J (1996) Radiosurgery for the treatment of previously irradiated primary brain tumors and brain metastasis: Initial report of Radiation Therapy Oncology Group Protocol 90–05. Int J Radiat Oncol Biol Phys 34:647–654
25. Shaw E, Scott C, Souhami L, Dinapoli R, Kline R, Loeffler J, Farnan N (2000) Single dose radiosurgical treatment of recurrent previously irradiated primary brain tumors and brain metastases: Final report of RTOG protocol 90–05. Int J Radiat Oncol Biol Phys 47:291–298

Neuroradiology (2007) 49:327–333
DOI 10.1007/s00234-006-0194-9

DIAGNOSTIC NEURORADIOLOGY

# Evaluation of pituitary macroadenomas with multidetector-row CT (MDCT): comparison with MR imaging

**Yukio Miki · Mitsunori Kanagaki · Jun A. Takahashi · Koichi Ishizu · Masayuki Nakagawa · Akira Yamamoto · Yasutaka Fushimi · Tsutomu Okada · Nobuhiro Mikuni · Ken-ichiro Kikuta · Nobuo Hashimoto · Kaori Togashi**

Received: 27 July 2006 / Accepted: 22 November 2006 / Published online: 3 January 2007


**Abstract**
*Introduction* It is important to have information on cavernous sinus extension and bony destruction in pituitary macroadenomas before surgery, but magnetic resonance (MR) imaging cannot always depict them. In the present study we sought to determine whether multidetector-row computed tomography (MDCT) could provide preoperative information in addition to that provided by MR imaging in pituitary macroadenoma.
*Methods* The subjects comprised 33 consecutive patients (15 women, 18 men; mean age 50 years) with surgically proven macroadenoma. For MDCT, using the soft-tissue window and bone window, three orthogonal multiplanar reconstruction images were generated from venous-phase contrast-enhanced 0.5-mm isotropic voxel data. MDCT and MR images were evaluated with regard to: (1) clarity of tumor margins; (2) identification of the normal pituitary gland; (3) identification of erosion or destruction of the sellar floor; and (4) visualization of the adjacent optic pathways.
*Results* MDCT more clearly demonstrated the lateral tumor margin than MR imaging ($P$=0.002). No significant differences in visualization of the normal pituitary gland were noted between MDCT and dynamic MR imaging ($P$=0.7). MDCT more clearly demonstrated sellar floor erosion or destruction at the sphenoid sinus than MR imaging ($P$< 0.001). MR imaging was superior to MDCT for visualizing the adjacent optic pathways ($P$<0.001).
*Conclusion* MDCT is superior to MR imaging for assessing lateral tumor margin and the sellar floor at the sphenoid sinus. MDCT offers useful preoperative information in addition to that obtained from MR imaging.

**Keywords** Pituitary adenoma · Multislice CT · MR imaging

Y.M. and M.K. contributed equally to this study.

Y. Miki (✉) · M. Kanagaki · K. Ishizu · A. Yamamoto · Y. Fushimi · T. Okada · K. Togashi
Department of Diagnostic Imaging and Nuclear Medicine, Graduate School of Medicine, Kyoto University, 54 Shogoin Kawahara-cho, Sakyo-ku, Kyoto 606-8507, Japan
e-mail: mikiy@kuhp.kyoto-u.ac.jp

J. A. Takahashi · N. Mikuni · K.-i. Kikuta · N. Hashimoto
Department of Neurosurgery, Graduate School of Medicine, Kyoto University, 54 Shogoin Kawahara-cho, Sakyo-ku, Kyoto 606-8507, Japan

M. Nakagawa
Department of Radiology and Nuclear Medicine Service, Kyoto University Hospital, 54 Shogoin Kawahara-cho, Sakyo-ku, Kyoto 606-8507, Japan

## Introduction

Up to the late 1980s, computed tomography (CT) was as the primary diagnostic imaging modality for pituitary macroadenoma. However, since its introduction magnetic resonance (MR) imaging has been used to obtain clinically useful preoperative information on this tumor [1–3]. The information provided by MR imaging in macroadenomas includes size and shape of the tumor, the presence of cavernous sinus extension, positional relationships with the optic pathways, identification of the normal pituitary gland, and the presence of hemorrhage or cyst within the tumor [2,

4]. CT is also still performed to assess the anatomy and condition of the nasal cavity and sphenoid sinus, which are crucial information for transsphenoidal surgery [2, 5–8]. Several investigators have compared CT and MR imaging in diagnosing pituitary macroadenoma. MR imaging can provide better soft-tissue contrast than CT, and also permits scanning in any desired plane [9–11].

The recent introduction of multidetector-row CT (MDCT) has allowed the acquisition of high-resolution images within a short time [12, 13]. Several studies have examined the usefulness of MDCT of the head for CT angiography, for evaluation of facial bone fractures, and for multislice perfusion imaging with high-speed continuous scanning [14–16]. MDCT images can be reconstructed in any desired plane from isotropic voxel data for morphological evaluation of tumors and tumor invasion, in addition to normal structures such as blood vessels and bones. While many reports have described the usefulness of MDCT for preoperative evaluation of neoplasms, most have focused on abdominal tumors [17, 18]. Abe et al. have reported the use of MDCT instead of MR imaging in pituitary adenoma in three patients with a pacemaker [19], but to the best of our knowledge, no studies have compared MDCT and MR imaging in pituitary macroadenoma. Since parasellar bony and vascular structures must be fully investigated prior to surgery for pituitary adenoma [5, 20], MDCT may be able to provide more detailed preoperative information than other imaging modalities. In the present study we sought to determine whether MDCT could provide preoperative information in addition to that provided by MR imaging in pituitary macroadenoma.

## Methods

### Patient population

The study population comprised 33 consecutive patients (15 men, 18 women) with pituitary macroadenoma (>10 mm in diameter) admitted to the Neurosurgical Department of our institution for surgery and examined prospectively using MDCT and MR imaging during the 4 weeks before surgery. Their mean age was 50 years (range 16 to 70 years). The tumors included nonfunctioning adenoma ($n$=20), growth hormone-producing adenoma ($n$=10), and prolactinoma ($n$=3). Patients who had undergone previous surgery for pituitary adenoma were excluded from the study. The present investigation was conducted in accordance with the guidelines of our institutional review board. Approval of the local institutional ethics committee for this study was considered unnecessary because the CT examinations had already been routinely performed as a preoperative evaluation of pituitary adenoma in our institution since it reportedly provides crucial information for transsphenoidal surgery [2, 5–8]. Written informed consent was obtained from all patients.

### MDCT protocols

CT scanning was performed using an eight-detector row CT scanner (Aquilion; Toshiba Medical, Tokyo, Japan). After placing a 20-gauge catheter in an antecubital vein, 100 ml of nonionic contrast material with an iodine content of 350 mg/ml (iomeprol, Iomeron Eisai, Tokyo, Japan) was injected at 3 ml/s using an automatic power injector (Dualshot; Nemoto-kyorindo, Tokyo, Japan). Scanning centered on the sella turcica was performed 80 s after initiation of the injection. This delay time (80 s) was chosen because the highest contrast between adenoma and normal pituitary tissue is achieved between 1 and 2 min after injection of contrast material, and because the cavernous sinus is well enhanced at this moment, according to data obtained with dynamic MR imaging [4, 21]. Parameters for the scanning were: 120 kVp, 300 mA, 8×0.5-mm collimation, rotation time 1.0 s, helical pitch 7, FOV 210 mm, matrix size 512×512.

Multiplanar reconstruction (MPR) soft-tissue window images were generated in the coronal (Fig. 1a), axial (Fig. 1b), and sagittal (Fig. 1c) planes with a slice thickness of 1.1 mm and an FOV of 80 mm by 0.3-mm interpolation. In addition, MPR bone window images were generated in the coronal (Fig. 2a), axial, and sagittal (Fig. 2b) planes with 1.1-mm slice thickness and an FOV of 125 mm by 0.3-mm interpolation. Data were transferred to a stand-alone workstation (Zio M900; ZIOSOFT, Tokyo, Japan) for evaluation using the software installed in the workstation.

### MR protocols

MR imaging was performed using a 1.5-T system (Magnetom Symphony; Siemens, Erlangen, Germany). Before contrast agent administration, T1-weighted sagittal and coronal images using spin-echo (SE) sequences (TR/TE 400/14 ms, matrix 256×192, FOV 180 mm, slice thickness 3 mm without interslice gap), and T2-weighted coronal images using fast spin-echo (FSE) sequences (TR/TE 4000/90 ms, matrix 256×192, echo train length 16, FOV 180 mm, slice thickness 3 mm without interslice gap) were obtained.

Dynamic images were acquired in the coronal plane using FSE sequences (TR/TE 500/12 ms, matrix 256×192, echo train length 8, FOV 180 mm, acquisition time 13 s). Four contiguous 3-mm-thick sections were obtained simultaneously. Dynamic imaging started with the first precontrast image, followed by a second image 15 s after

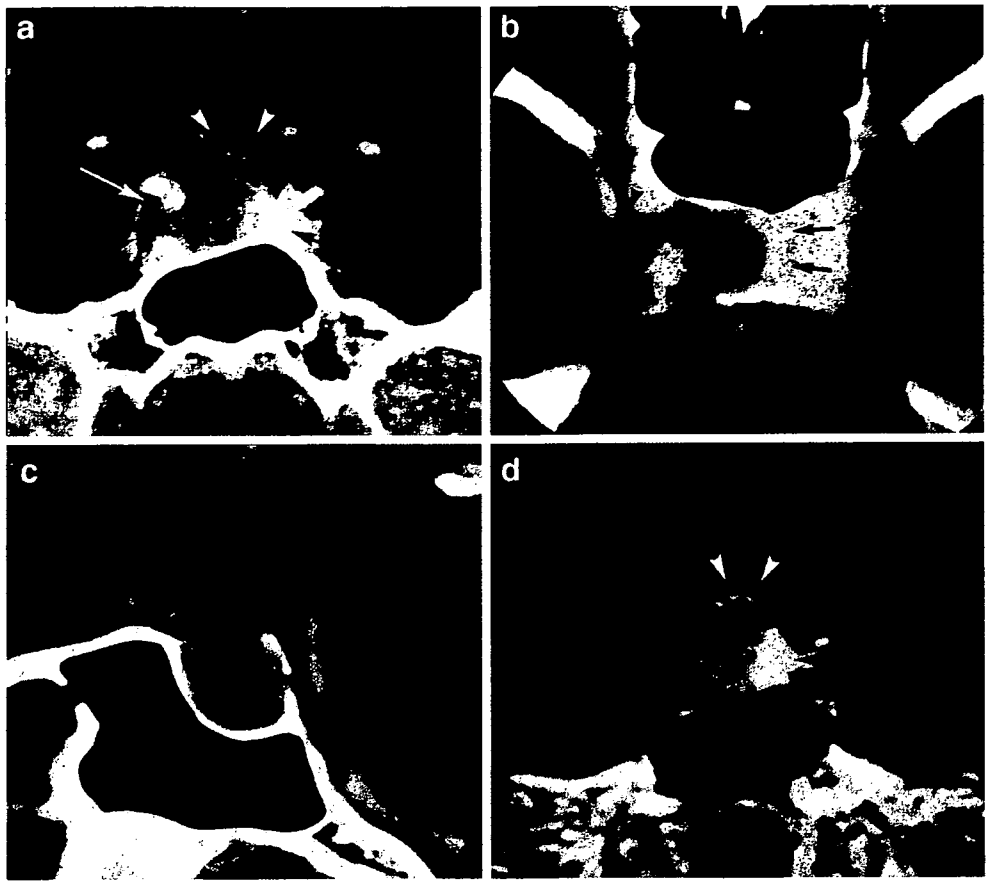


**Fig. 1** Nonfunctioning pituitary macroadenoma invading the right cavernous sinus, which was confirmed by surgery. Three orthogonal soft-tissue window contrast-enhanced MDCT images are shown (**a–c**). MDCT clearly demonstrates the lateral margin of the tumor in the right cavernous sinus (*black arrowheads*) (**a**, **b**). The compressed pituitary gland is clearly identified on the left side of the hypophyseal fossa both on MDCT (score 2) and dynamic MR image (score 2) (*black arrows*) (**a**, **b**, **d**). The tumor margins in the cavernous sinus are more clearly depicted on MDCT (score 2) (**a**, **b**) (*black arrowheads*) than on the dynamic T1-weighted MR image (score 1) (**d**). The optic chiasm is better demonstrated by MR imaging (score 2) (**d**) than by MDCT (score 1) (**a**) (*white arrowheads*). *White arrow* oculomotor nerve (**a**)

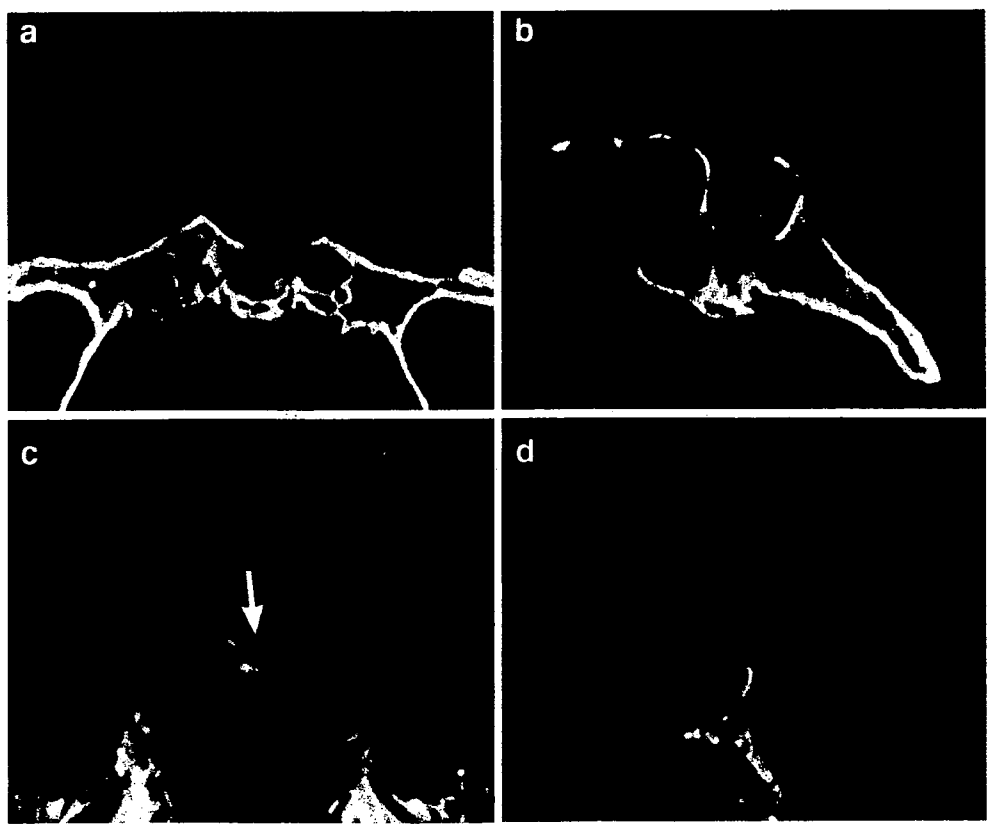


**Fig. 2** Growth hormone-producing pituitary adenoma eroding the floor of the sella turcica and invading the sphenoid sinus and clivus. Coronal and sagittal bone window reconstructed MDCT images (score 2) (**a**, **b**) demonstrate destruction of the sellar floor better than coronal and sagittal spin-echo T1-weighted MR images (score 1) (**c**, **d**) (*arrows*)

the start of rapid injection (4 ml/s) of 0.05-mmol/kg gadopentetate dimeglumine (gadodiamide, Omniscan; Daiichi Pharmaceutical, Tokyo, Japan), with five subsequent serial images obtained over 90 s at 15-s intervals (30, 45, 60, 75 and 90 s). Gadolinium-enhanced T1-weighted coronal images (SE, TR/TE 500/12 ms, matrix 256×192, FOV 180 mm, slice thickness 3 mm without interslice gap) were also obtained. These data were also transferred to the workstation.

### Image analysis

The images were independently analyzed by two experienced neuroradiologists. Any discrepancies between the two scorers were discussed until a consensus was reached. MDCT and MR images were evaluated with regard to the following points required for preoperative evaluation: (1) clarity of lateral tumor margins; (2) identification of the normal pituitary gland; (3) identification of the presence of erosion or destruction of the sellar floor; and (4) visualization of the neighboring optic pathways.

### Clarity of lateral tumor margins

Coronal reconstructed soft-tissue window MDCT images were compared with coronal MR images with regard to visualization of lateral tumor margins. The clarity of the lateral tumor margins was graded using a three-grade scale: 0, tumor margins not clearly visualized; 1, tumor margins visualized, but some discontinuities observed; and 2, tumor margins visualized with no discontinuities.

### Identification of the normal pituitary gland

Coronal reconstructed soft-tissue window MDCT images were compared with delayed-phase images of the coronal T1-weighted dynamic MR study with regard to identification of the normal pituitary gland using a three-grade scale: 0, normal pituitary gland not identified; 1, normal pituitary gland identified with high probability; and 2, normal pituitary gland definitely identified.

### Erosion or destruction of the sellar floor

Sagittal and coronal reconstructed bone-window MDCT images were compared with sagittal and coronal T1-weighted MR images with regard to visualization of erosion or destruction of the sellar floor using a two point scale: 0, bony structures with or without erosion or destruction not clearly visualized; 1, bony structures with or without erosion or destruction clearly visualized. Erosion or destruction of the sellar floor was evaluated at the sphenoid sinus and into the clivus, respectively.

### Visualization of neighboring optic pathways

Coronal reconstructed soft-tissue window MDCT images were compared with coronal T1-weighted MR images with regard to visualization of neighboring optic pathways using a three-grade scale: 0, neighboring optic pathways not visualized; 1, neighboring optic pathways partially visualized; and 2, neighboring optic pathways clearly visualized.

### Statistical analysis

Differences between MDCT and MR imaging findings were assessed using the Wilcoxon signed ranks test with JMP 5.0 software (SAS Institute, NC). $P$ values $<0.05$ were considered statistically significant.

## Results

### Clarity of lateral tumor margins

For lateral tumor margins, MDCT yielded grade 2 results in 32 of 33 patients (97%) and grade 1 results in 1 of 33 patients (3%), while MR imaging yielded grade 2 results in 22 of 33 patients (67%) and grade 1 results in 11 of 33 patients (33%). MDCT visualized the lateral tumor margin significantly better than MR imaging ($P$=0.002; Fig. 1a,d). Surgery confirmed the presence or absence of cavernous sinus invasion in 28 patients (all the 13 patients with hormone-secreting adenoma and 15 of the 20 patients with nonfunctioning adenoma). Of these 28 patients, 13 were confirmed to have cavernous sinus invasion. MDCT yielded grade 2 results in all these 13 patients, and MRI yielded grade 2 results in 11 patients and grade 1 results in 2 patients.

### Identification of the normal pituitary gland

The presence of normal pituitary gland was definitely identified (grade 2) in 22 of 33 patients (67%) by both MDCT and dynamic MR imaging. Normal pituitary gland was identified with high probability (grade 1) in 5 of 33 patients (15%) by MDCT and in 7 of 33 patients (21%) by dynamic MR imaging. No significant difference in identification of normal pituitary gland was observed between the two modalities ($P$=0.7; Fig. 1a,d). Surgery revealed normal pituitary gland at the suspected locations in 28 of 33 patients (85%).

### Erosion or destruction of the sellar floor

*At the sphenoid sinus* Bony structures with or without erosion or destruction were clearly visualized in all 33

patients (100%) by MDCT and in 19 patients (58%) by MR imaging. MR imaging could not distinguish between bony destruction and ballooning of the sellar floor in the remaining 14 patients (42%). Erosion or destruction of the sellar floor was visualized significantly better with MDCT than with MR imaging ($P<0.001$; Fig. 2).

*Into the clivus* Bony structures with or without erosion or destruction were clearly visualized in 32 patients (97%) by MDCT and in 27 patients (82%) by MR imaging. There was no statistically significant difference between the two modalities regarding visualization of erosion or destruction of the sellar floor into the clivus ($P=1.0$).

Visualization of the adjacent optic pathways

Adjacent optic pathways were clearly visualized (grade 2) in 20 of 33 cases (61%), were not clearly visualized in some areas (grade 1) in 12 of 33 patients (36%), and not visualized (grade 0) in 1 of 33 patients (3%) with MR imaging. Grade 2 visualization of the adjacent optic pathways was achieved in no patients, grade 1 in 2 of 33 patients (6%), and grade 0 in 31 of 33 patients (94%) on MDCT. MR imaging visualized adjacent optic pathways significantly better than MDCT ($P<0.001$; Fig. 1a,d).

## Discussion

The present study revealed that MDCT is superior to MR imaging for visualizing the lateral tumor margin, and for providing accurate depiction of bony structures. To our knowledge, this is the first study to reveal the usefulness of MDCT in pituitary adenomas in comparison to MR imaging.

MDCT was superior to MR imaging for determining the lateral tumor margin ($P=0.002$). Macroadenomas frequently invade the cavernous sinus, and preoperative evaluation of the presence and degree of cavernous sinus extension is important to ensure that the tumor within the cavernous sinus can be safely resected during transsphenoidal surgery. However, neither CT nor MR imaging has been able to directly depict the walls of the cavernous sinus [22–25]. Thus, cavernous sinus extension has been assessed indirectly based on relationships between tumor margins and normal structures such as the internal carotid artery within the cavernous sinus [22]. Accurate visualization of tumor margins is therefore crucial to determine whether cavernous sinus extension is present. In this study, the lateral tumor margins were visualized with no discontinuities in 97% of patients.

The present study also revealed that MDCT is comparable to dynamic MR imaging in identifying the normal pituitary gland. Dynamic MR imaging has been reported to be useful in visualizing the normal pituitary gland in patients with pituitary macroadenoma [4]. Identifying the normal pituitary gland before surgery is clinically important. The normal pituitary gland cannot always be identified during surgery for pituitary macroadenoma, but if the location can be estimated preoperatively, surgery can be performed such that damage to the pituitary gland is avoided, thus minimizing the risk of hypopituitarism and promoting the recovery of normal endocrine function [26].

Erosion or destruction of the sellar floor at the sphenoid sinus was better visualized with MDCT than with MR imaging ($P<0.001$), although there was no significant difference regarding evaluation of erosion or destruction of the sellar floor into the clivus between the two modalities ($P=1.0$). Sagittal and coronal MDCT bone-window images clearly depicted erosion or destruction of the sellar floor by the tumor. MDCT with thin-slice collimation can clearly depict three-dimensional changes in bony structures [15]. In contrast, MR imaging cannot directly visualize bone cortices or trabeculae, so distinguishing between thinning and a defect of the ballooned sellar floor at the sphenoid sinus is difficult, although MR images can visualize the bone marrow in the clivus. With regard to hormone-producing adenomas, which must be resected to the greatest extent possible, evaluating the direction and degree of bony invasion is crucial. Moreover, bone-window MPR MDCT images are useful not only for identifying bone invasion by the tumor, but also for evaluating variations in the nasal cavity and paranasal sinuses, which are located along the surgical route in transsphenoidal surgery. In particular, bone-window MPR images permit precise morphological evaluation of the sphenoid sinus, which is required for assessing the approach to the sella turcica. MPR images may therefore be useful for surgical mapping.

MR imaging was significantly superior for evaluating positional relationships between the tumor and the optic pathways ($P<0.001$). Compared with MR imaging, CT offers inferior contrast resolution between CSF and soft tissues, and is of limited use for small structures such as the optic nerve and optic tract [27]. Since optic pathway injury represents a serious surgical complication, precise preoperative evaluation of positional relationships between tumor and neighboring optic pathways is essential. In this regard, MDCT is inferior to MR imaging.

Radiation exposure from CT examination might be a matter of concern. As a preoperative evaluation of pituitary adenoma (especially for transsphenoidal surgery), CT is already commonly performed so that neurosurgeons can know the detail of bony structures of the sphenoid sinus and nasal cavity preoperatively [2, 5–8]. Thus, application of MDCT in pituitary adenomas will not generate additional CT examinations. We believe that patients will not be

exposed to significant additional radiation if CT examination is performed only as a preoperative examination as in this study. Regarding radiation exposure from CT examination, the following two points should be emphasized: (1) MDCT must not be used for screening but in candidates for surgery; (2) postcontrast CT is enough (without a precontrast study) for delineating both tumor margin and bony changes.

There are some limitations to this study. First, the presence or absence of cavernous sinus invasion was not surgically confirmed in some patients with a non-functioning adenoma. Second, the location of the normal pituitary gland was not surgically confirmed in all the patients. Since pituitary adenoma is rarely life-threatening, the objective of surgery is to improve or maintain visual function and endocrine function. In particular, the objectives of surgery for non-functioning adenoma are to improve clinical symptoms by debulking the tumor, rather than removing the entire tumor. Therefore, aggressive surgery was not performed in order to avoid damage to the normal pituitary gland and bleeding. As a result, the presence or absence of cavernous invasion or the location of the normal pituitary gland was not confirmed during surgery in all patients. No patient showed deterioration of pituitary endocrine function following surgery in the present study. The third limitation of the current study is that patients with microadenoma were not included, since microadenomas do not invade the cavernous sinus nor destroy the sellar floor as frequently as macroadenomas do. The usefulness of MDCT in microadenoma may be evaluated in the future.

## Conclusion

MDCT is superior to MR imaging for providing information concerning the lateral tumor margin and the sellar floor at the sphenoid sinus in pituitary macroadenoma. MDCT can thus offer useful information in addition to that obtained from MR imaging for surgical planning.

**Conflict of interest statement** We declare that we have no conflict of interest.

## References


1. Kucharczyk W, Davis DO, Kelly WM, Sze G, Norman D, Newton TH (1986) Pituitary adenomas: high-resolution MR imaging at 1.5 T. Radiology 161:761–765
2. Elster AD (1993) Modern imaging of the pituitary. Radiology 187:1–14
3. Korogi Y, Takahashi M (1995) Current concepts of imaging in patients with pituitary/hypothalamic dysfunction. Semin Ultrasound CT MRI 16:270–278
4. Miki Y, Matsuo M, Nishizawa S, Kuroda Y, Keyaki A, Makita Y, Kawamura J (1990) Pituitary adenomas and normal pituitary tissue: enhancement patterns on gadopentetate-enhanced MR imaging. Radiology 177:35–38
5. Saeki N, Yamaura A, Numata T, Hoshi S (1999) Bone window CT evaluation of the nasal cavity for the transsphenoidal approach. Br J Neurosurg 13:285–289
6. Saeki N, Iuchi T, Higuchi Y, Uchino Y, Murai H, Isono S, Yasuda T, Minagawa M, Yamaura A, Sunami K (2000) Bone CT evaluation of nasal cavity of acromegalics – its morphological and surgical implication in comparison to non-acromegalics. Endocr J 47 Suppl:S65–S68
7. Abe T, Asahina N, Kunii N, Ikeda H, Izumiyama H (2003) Usefulness of bone window CT images parallel to the transnasal surgical route for pituitary disorders. Acta Neurochir (Wien) 145:127–131
8. Naim UR, Jamjoom A, Jamjoom ZA (1996) Modified coronal computerized tomographic cuts for transsphenoidal surgery. Technical note. Neurosurg Rev 19:85–88
9. Davis PC, Hoffman JC Jr, Spencer T, Tindall GT, Braun IF (1987) MR imaging of pituitary adenoma: CT, clinical, and surgical correlation. AJR Am J Roentgenol 148:797–802
10. Lundin P, Bergstrom K, Thuomas KA, Lundberg PO, Muhr C (1991) Comparison of MR imaging and CT in pituitary macroadenomas. Acta Radiol 32:189–196
11. Kulkarni MV, Lee KF, McArdle CB, Yeakley JW, Haar FL (1988) 1.5-T MR imaging of pituitary microadenomas: technical considerations and CT correlation. AJNR Am J Neuroradiol 9:5–11
12. Nieman K, Oudkerk M, Rensing BJ, van Ooijen P, Munne A, van Geuns RJ, de Feyter PJ (2001) Coronary angiography with multislice computed tomography. Lancet 357:599–603
13. Schroeder T, Nadalin S, Stattaus J, Debatin JF, Malago M, Ruehm SG (2002) Potential living liver donors: evaluation with an all-in-one protocol with multi-detector row CT. Radiology 224:586–591
14. Kudo K, Terae S, Katoh C, Oka M, Shiga T, Tamaki N, Miyasaka K (2003) Quantitative cerebral blood flow measurement with dynamic perfusion CT using the vascular-pixel elimination method: comparison with H2(15)O positron emission tomography. AJNR Am J Neuroradiol 24:419–426
15. Philipp MO, Funovics MA, Mann FA, Herneth AM, Fuchsjaeger MH, Grabenwoeger F, Lechner G, Metz VM (2003) Four-channel multidetector CT in facial fractures: do we need 2×0.5 mm collimation? AJR Am J Roentgenol 180:1707–1713
16. Jayaraman MV, Mayo-Smith WW, Tung GA, Haas RA, Rogg JM, Mehta NR, Doberstein CE (2004) Detection of intracranial aneurysms: multi-detector row CT angiography compared with DSA. Radiology 230:510–518
17. Sheth S, Scatarige JC, Horton KM, Corl FM, Fishman EK (2001) Current concepts in the diagnosis and management of renal cell carcinoma: role of multidetector CT and three-dimensional CT. Radiographics 21 Spec No:S237–S254
18. Prokesch RW, Chow LC, Beaulieu CF, Nino-Murcia M, Mindelzun RE, Bammer R, Huang J, Jeffrey RB Jr (2002) Local staging of pancreatic carcinoma with multi-detector row CT: use of curved planar reformations initial experience. Radiology 225:759–765
19. Abe T, Izumiyama H, Fujisawa I (2002) Evaluation of pituitary adenomas by multidirectional multislice dynamic CT. Acta Radiol 43:556–559
20. Weir B (1992) Pituitary tumors and aneurysms: case report and review of the literature. Neurosurgery 30:585–591
21. Korogi Y, Takahashi M, Sakamoto Y, Shinzato J (1991) Cavernous sinus: correlation between anatomic and dynamic gadolinium-enhanced MR imaging findings. Radiology 180:235–237